# Probing cosmic monsters: confronting hydrodynamic simulations with new observations of high-density environments

Ahad, S.L.

# 1

# Introduction



## 1.1 Our understanding of the Universe: A brief history

Similar to the development of human civilization, our progress in understanding the Universe and our place in it, has made the biggest leaps in the last few centuries compared to the last few millennia and in the last few decades compared to the last few centuries. Not surprisingly, our understanding of the Universe improved in tandem with the advent and availability of new technology. Only a few hundred years ago, the first use of a refractive telescope to look at the skies showed that Jupiter and Saturn also have moons orbiting them, challenging the long-standing Earth-centric model of the Universe before that. A few centuries later, less than a hundred years ago, Edwin Hubble used the 100-inch telescope at Mount Wilson Observatory to measure distances of variable stars in M31 and M33 by using the period-luminosity relations of Cepheid variable stars. He demonstrated that the fuzzy cloud-like 'nebulae' in the night sky were indeed very large systems that were very far away. This was the first proof that our Milky Way is not the only 'island' of stars or 'galaxy' in the Universe, but rather one of many. In Western culture, the name 'galaxy' comes from the Greek word $\gamma\acute{\alpha}\lambda\alpha$, which means milk, referring to the fuzzy and milky appearance of the Milky Way[1]. From naming our Galaxy after some spilt milk in the sky to understanding that these stars are not the only objects in the Universe, rather we are in a galaxy like many others, took us thousands of years. However, from realizing that there are other galaxies to finding hundreds of other galaxies and classifying them into types took only a few. Based on how the galaxies appear in optical images, or what we call galaxy morphology, Hubble proposed a classification of galaxies following a progression from simple (Spherical/Elliptical) to more complex (spirals/barred spirals) forms, which

[1]The name Milky Way is derived from its classical Latin term 'via lactea', which is translated from the Hellenistic Greek term $\gamma\alpha\lambda\alpha\xi\acute{\iota}\alpha\varsigma\ \kappa\acute{\upsilon}\kappa\lambda\circ\varsigma$ (galaxías kýklos), meaning 'milky circle'.

was possible through the use of the biggest telescope at that time. Soon after, in 1927-1929, based on the measured distances from Hubble and redshifts from Slipher (1917), Hubble and Lemaître linked that all these galaxies are moving away from us, and their receding velocities are proportional to their distances from us[2]. Detailed discussions of pre-1929 observations leading to this conclusion can be found in Trimble (2012) and Trimble (2013). This discovery drastically changed yet another idea about our Universe: it is expanding over time instead of being static as previously thought of because of the apparent static location of stars in the sky. This discovery brought humankind's long-held question of 'where did everything come from' from a pure theoretical practice into the realm of data-driven science, providing a crucial clue to guide the theory of modern Cosmology as we know it today.



## 1.2 The Standard Model of Cosmology

The current Standard Model of Cosmology, also called the 'Concordance Cosmological Model' or the 'Lambda Cold Dark Matter (ΛCDM) Model', is one of the best achievements of modern science, both theoretically and observationally, albeit with several loose ends including the reliance on untested theories about inflation, dark matter, and dark energy. The primary assumption of this model is the 'cosmological principle', which states that the Universe is homogeneous and isotropic on sufficiently large scales. Based on the framework of Einstein's general theory of relativity (GTR) and the cosmological principle, the metric describing space-time and determining the distances separating nearby points ( e.g., stars, galaxies) is the Friedmann-Lemaître-Robertson-Walker metric (FLRW metric). Friedman (1922) solved the field equations of GTR by assuming the cosmological principle. A similar result was obtained by Lemaître (1927). Most of the solutions of the Friedmann field equations predict an expanding or contracting universe, depending upon initial parameters such as the mass-energy of the universe.

Discovery of the Hubble-Lemaître law (Hubble, 1929) implied that (i) only the expanding solutions of the Friedmann equations are allowed as solutions for the Universe and (ii) the universe must have had a very dense and hot beginning, motivating the Big Bang model, an important element in our current understanding of the Universe.

According to the ΛCDM cosmology model, the mass-energy budget of the Universe is distributed mainly between the invisible but gravitationally interacting 'dark'

[2]Previously known as the Hubble Law. In 2018, the International Astronomical Union resolved it to be referred to as the Hubble-Lemaître law

matter ($\approx$ 25%) and an even more mysterious 'dark energy' ($\approx$ 70%), leaving only $\approx$ 5% to ordinary matter that includes all the elements in the periodic table (Planck Collaboration XVI, 2014; Planck Collaboration et al., 2020).



So far, we have only found indirect evidence of the presence of dark matter and dark energy. Oort (1932) inferred missing matter in the Solar neighbourhood from the velocity of stars. However, the first indirect observation of dark matter is usually attributed to Fritz Zwicky in 1933 (e.g. Trimble 1987; Einasto 2013). By studying the motion of galaxies in the Coma cluster of galaxies, Zwicky (1933) found that these galaxies move faster than the expected velocities their total visible mass could gravitationally hold, and inferred that there must be more (10 to 100 times) mass in that system than the amount we can estimate from the visible light. Several decades later, through a study of the rotation velocity of stars in spiral galaxies, Rubin and Ford (1970) and Rubin et al. (1980) also reported that most of the gravitational matter in galaxies could not be observed, providing a sign of dark matter on the galaxy scale.

The first observational evidence of dark energy came from another surprising discovery. Through the study of distant type Ia supernovae, Riess et al. (1998) and Perlmutter et al. (1999) found that the expansion of the Universe is accelerated. We use the term 'dark energy' to refer to the cause of this acceleration, and the '$\Lambda$' term was added in the $\Lambda$CDM model to represent it.

The $\Lambda$CDM model is supported by several other empirical pillars, including (i) the primordial nucleosynthesis (Alpher et al., 1948), i.e. the formation theory of the light elements (Hydrogen, Helium, Lithium) very soon following the Big Bang and the fact that the quantitative predictions from this theory agree extremely well with observations, (ii) the discovery of the cosmic microwave background radiation (CMBR) by Penzias and Wilson (1965). The CMB is predicted by the hot Big Bang hypothesis (Dicke et al., 1965), being the afterglow with very small temperature fluctuation ($dT/T \approx 10^{-5}$) approximately 380,000 years after the Big Bang. (iii) the development of the inflationary model that explains the homogeneity of the CMB with a brief period of exponential size growth of the very early Universe (Guth, 1981). Since its discovery in 1965, the CMB, in particular, has been studied with continuously improved measurements from multiple observational programs (COBE - Bennett et al. 1996, WMAP - Bennett et al. 2003, Planck - Planck Collaboration et al. 2020) and has been the most constraining probe of the standard cosmology model.

The $\Lambda$CDM model of cosmology has been, so far, the most evidence-supported model of the Universe. However, there are still several missing elements, especially our lack of understanding about the nature of the dominant components of the Uni-

verse, dark energy and dark matter. While many current and upcoming efforts are ongoing to understand the nature of these components, there is also room for alternative theories, such as a different type of dark matter other than the 'cold dark matter' or an alternative theory to explain gravity other than the GTR.



## 1.3 Hierarchical structure formation

According to the Big Bang theory in the ΛCDM paradigm, the extrapolation of the expansion of the Universe backwards in time yields an approximation of the time when it all started, about 13.8 billion years ago. Just after the Big Bang, all the matter in the Universe was hot, dense, ionised, and remarkably homogeneously distributed. We see an imprint of this matter density distribution of the early Universe in the nearly isotropic temperature of the CMB. However, the density distribution also had very small inhomogeneities, which we see in the small-scale temperature fluctuations of the CMB. From that (nearly) smooth distribution, the transition into the current distribution of galaxies in the Universe as we observe (e.g. Colless et al. 2001) started with these very small initial density perturbations in the early Universe.

While the thermal photons interacted with the baryonic matter and kept them in a fluid-like form with complex oscillatory behaviour (Peebles and Yu, 1970), the non-interacting dark matter could clump together due to gravity, increasing the amplitude of the primordial density fluctuations. These small density fluctuations then grew larger under the influence of gravity over time, eventually initiating gravitational collapse and forming dark matter haloes (e.g. Peacock 1999; Delos and White 2023). The hot, ionized baryons remained tightly coupled to the radiation field and could not collapse further until the Universe cooled sufficiently. At this point, about 100 million years after the Big Bang, the baryons were able to collapse into the early dark matter haloes and formed the first stars that subsequently created the first galaxies (Press and Schechter, 1974; White and Rees, 1978; Mo et al., 2010).

At present, galaxies in the Universe are not distributed randomly, but in a complex web-like structure with voids, filaments, and at the junction of the latter – nodes, which is known as the Cosmic Web structure. This large-scale structure of the Universe is observed in large galaxy surveys like the 2DF survey (Colless et al., 2001) and the Sloan Digital Sky Survey (SDSS; York et al. 2000). As the Universe is, to first order, governed by gravity (especially when dark matter dominates), we can evolve the primordial dark

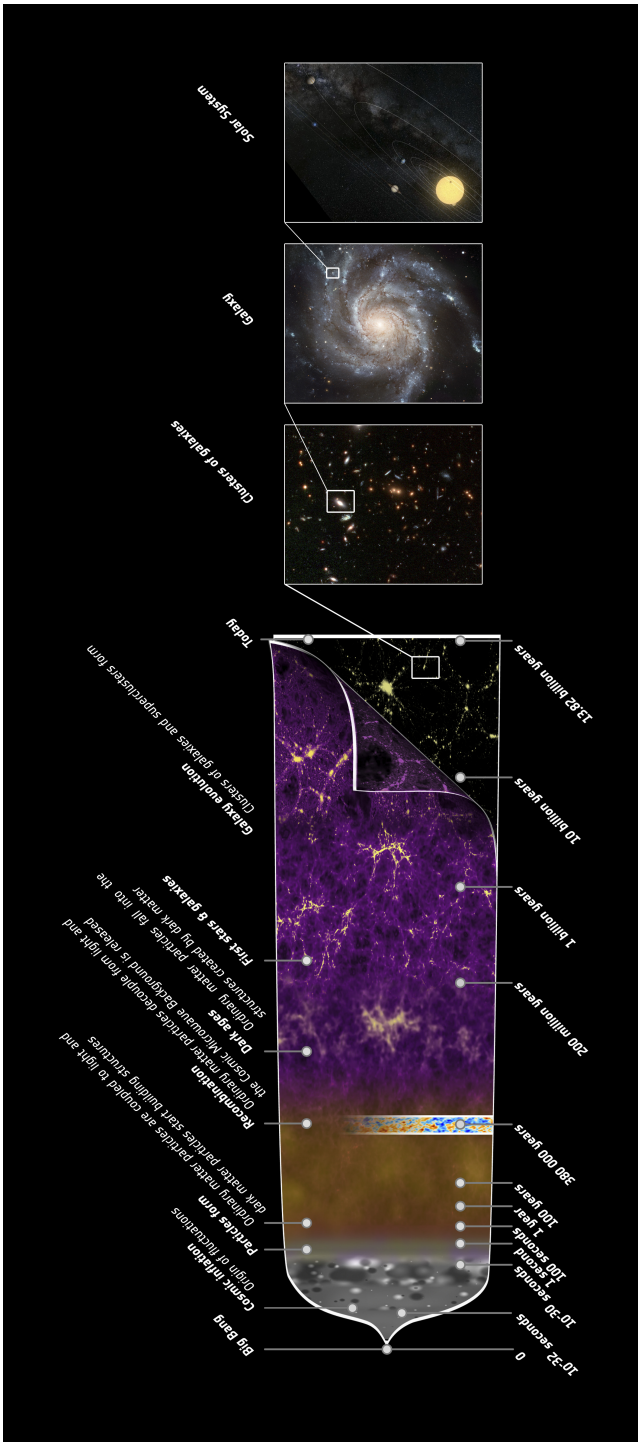


**Figure 1.1:** Timeline of the Universe from the beginning through the 13.8 billion-year history. It shows the main events that occurred between the initial small density fluctuations and the rich variety of galaxies that we observe today. The panels on the right side zoom into the large-scale structures to reveal a cluster of galaxies, a spiral galaxy, and the Solar System, respectively. Figure from ESA/Planck.

matter fluctuations to present days under the influence of gravitational force using numerical N-body simulations, which reproduce similar cosmic web-like structures to the observations (e.g., Springel et al. 2005). The formation of stars and evolution of galaxies in the dark matter haloes of these galaxies, however, follows complex baryonic physics. A central question of modern extragalactic astronomy is to understand a complete picture of the complex processes that transform the hot ionized gas in dark matter haloes into the diverse types of galaxies that populate our Universe now.

From the first stars to the Cosmic Web, the growth of the large-scale structure of the Universe can be explained in a hierarchical formation scenario (an illustration of the timeline of the Universe is provided in Fig. 1.1). In the early Universe, the typical masses of the dark matter haloes were small, but they grew hierarchically with cosmic time through merging with other haloes and accretion of diffuse dark matter. This is also observed in the aforementioned N-body simulations. Galaxies formed within these dark matter haloes and aggregated along the already existing interconnected cosmic filaments of dark matter, eventually leading to the formation of massive galaxy clusters at the intersections of filaments, making them the largest gravitationally bound structures in the Universe. Being the last-formed structures in the hierarchical formation model, their abundance and mass distributions are excellent tools to test the theory of structure formation over cosmic time. Moreover, the matter density and the expansion of the Universe regulate when such massive structures like galaxy clusters can form and how far apart they can be at different cosmic epochs. Therefore, the number density of clusters and their formation epochs can provide significant constraints on the nature of dark matter and dark energy. These parameters can be studied on a linear scale from the large-scale structure of the Universe. However, to constrain these measurements further, a detailed understanding of the formation and evolution of galaxy clusters and the galaxies within them is necessary. For more discussion on the formation of galaxy clusters and their role as cosmological probes, see e.g., Allen et al. (2011) and Kravtsov and Borgani (2012).

## 1.4 Galaxy evolution in high-density environments

Galaxy groups and clusters contain hundreds to thousands of galaxies in a small volume (1-2Mpc radius) compared to how galaxies are distributed in other areas along the large-scale structure. From small groups with halo mass $\sim 10^{12.5}\mathrm{M}_{\odot}$, to large clusters like the Coma cluster with $> 10^{15}\mathrm{M}_{\odot}$, these systems cover a wide mass range. Because of their dense distribution of galaxies, galaxy groups and clusters are unique cosmic

laboratories to study the impact of galaxy interactions and environment on galaxy formation. Many observational studies have been conducted on galaxy groups and clusters over the last 50+ years, and it is well-established that galaxy properties differ significantly between these dense systems and the average sparse galaxy distribution or the "field" environment. For example, at a fixed stellar mass, galaxies in denser environments are more likely to be elliptical in morphology (Dressler, 1980), have low levels of or no recent or ongoing star formation (Dressler, 1980; Balogh et al., 1999; Kauffmann et al., 2004; Weinmann et al., 2006; Blanton et al., 2005; Peng et al., 2010; Wetzel et al., 2012; Woo et al., 2012), and have a much lower amount of atomic hydrogen (e.g. Giovanelli and Haynes, 1985; Fabello et al., 2012; Hess and Wilcots, 2013; Odekon et al., 2016; Brown et al., 2017) in comparison with galaxies in the field.

Over the last decades, different physical mechanisms have been identified as potential causes of such differences in galaxy properties in groups and clusters compared to the field. A review of these can be found in Boselli and Gavazzi (2006) and Boselli et al. (2022). The hot halo of gas or the intracluster medium (ICM) can exert ram pressure on galaxies moving through it (Gunn and Gott, 1972; Larson et al., 1980; McCarthy et al., 2008). The ram pressure from the ICM can be strong enough to strip cold gas from a group/cluster galaxy and prevent further star formation (Gunn and Gott, 1972). Ram pressure may also trigger temporary star formation bursts in the galaxy (Tonnesen and Bryan, 2012) and consequently deplete it of available gas resources. If ram pressure is not efficient enough to strip the cold gas directly, it may still be able to remove the hot gas haloes in the circumgalactic medium (CGM). The hot CGM is expected to act as a reservoir that gradually replenishes the more centrally concentrated cold gas disc as it is used up by star formation (White and Rees, 1978; White and Frenk, 1991). Once the central cold gas is used up for star formation, losing the hot CGM will eventually quench the star formation. This process is referred to as 'strangulation' or 'starvation' (Larson et al. 1980, see also Balogh et al. 2000; McCarthy et al. 2008). Tidal forces due to the halo potential can temporarily increase the star formation activity of cluster galaxies by causing disc gas clouds to collide and collapse (Byrd and Valtonen, 1990). Such tidal forces can strip the haloes of gas, stars, and dark matter (e.g. Willman et al. 2004; Weinmann et al. 2010.

Besides the above-mentioned processes, frequent encounters between galaxies can also contribute to the observed diversity of galaxy morphology in dense environments (e.g. Merritt 1983). 'Galaxy harassment' or repeated rapid encounters in galaxy clusters can particularly impact the morphology of low surface brightness galaxies (Moore et al., 1996; Moore et al., 1998). Galaxy mergers and repetitive slow encounters be-

tween group members can form an elliptical galaxy from two spirals and also trigger temporary starbursts (e.g., Bekki and Couch 2011).

While our understanding of the processes that dominate galaxy evolution in dense environments has grown over the last decades, many open questions remain in our picture of how the interplay of these processes shapes the galaxy population in such environments. A few of such issues that are relevant to this thesis are discussed in the following section.



### 1.4.1 Some recent highlights of the field

In the local Universe, we can reproduce the assembly of galaxies in such a system with simplified galaxy evolution models (e.g., Peng et al., 2010, 2012; Wetzel et al., 2012), although a clear understanding of the processes is yet to be uncovered. Moreover, at higher redshifts ($z > 1$), these theories fail to explain some more recent observations. For example, from studying a set of 11 massive clusters at $1 < z < 1.5$ from the Gemini Observations of Galaxies in Rich Early Environments (GOGREEN) project (Balogh et al., 2017, 2021), van der Burg et al. (2020) found that the stellar mass function (SMF) of quenched galaxies has almost the same shape as in the average field environment at the same redshift. The existing galaxy quenching models based on the observations of the local Universe, such as the model from Peng et al. (2010) would predict them to look different. This is because the SMF of quenched galaxies in clusters is shaped by both self- (independent from the environment) and environment-dependent quenching processes, whereas field galaxies are only self-quenched. As long as there is any excess environment-induced quenching—such as in the GOGREEN clusters—the shapes of quenched SMFs of cluster and field galaxies should not look the same. In a different study, Webb et al. (2020) found that the mean stellar ages of these quenched massive galaxies from the GOGREEN clusters are about $0.31^{+0.51}_{-0.33}$ Gyr older than field galaxies at the same redshift at the stellar mass range $10^{10}$ – $10^{11.8}\mathrm{M}_{\odot}$, with an inferred quenching epoch at $z > 3$. If environmental quenching were significant for these massive cluster galaxies, one would instead expect them to have been quenched later than the field, and therefore have younger stellar populations, contrary to what is observed. Also, this happened in the proto-cluster era, when the ICM was still forming and unlikely to induce efficient ram-pressure stripping. Although some studies found evidence of ram-pressure stripping out to $z = 2$, whether it was strong enough to induce environmental quenching is still not resolved (for more discussion on this, see e.g. Boselli et al., 2022). These recent findings posed a new question: were galaxies

in field and dense environments fundamentally different in some of their aspects when clusters formed, or are they similar objects in different distributions as it seems based on observations in the local Universe? Galaxy evolution in high-redshift clusters and protoclusters, as well as cluster formation and growth in the protocluster era, are areas where we have many unanswered questions, and many future programs are being designed to investigate these.



Another recent area of focus in galaxy cluster study is the diffuse stellar halo around the central galaxies in groups and clusters, also known as the intragroup or intracluster light (IGL/ICL, for recent reviews, see e.g. Mihos, 2015; Montes, 2022)[3]. The ICL is essentially a fossil record of the galaxy interactions during the assembly of large-scale structures. Besides the galaxies in groups and clusters, ICL is generally considered as a separate stellar component of the host systems because it extends out to several hundreds of kilo-parsecs from the host centres and can envelop multiple galaxies in the host system. The radial extent of ICL around central galaxies in groups and clusters and the contribution of the ICL in the total light from these systems can provide important constraints for cosmic structure formation and assembly of giant elliptical galaxies. Due to its diffuse nature, the study of ICL falls into the low-surface brightness ($\mu \geq 27$ mag/arcsec$^2$) regime, which is one of the last remaining frontiers of observational optical astronomy. With the availability of deep multi-band photometry, there have been increasing efforts to study the ICL in individual clusters (e.g. Mihos et al., 2005; Montes and Trujillo, 2014, 2018; Jiménez-Teja et al., 2018; DeMaio et al., 2018, 2020; Montes et al., 2021; Martínez-Lombilla et al., 2023; Ragusa et al., 2023). Another way to account for the low signal-to-noise ratio in ICL analysis is to stack a large sample of groups/clusters from large surveys (e.g. Zibetti et al., 2005; Zhang et al., 2019).

The origin and growth of the ICL have been connected to multiple formation scenarios, including galaxy mergers (Murante et al., 2007), tidal stripping (Gallagher and Ostriker, 1972), galaxy disruption (Guo et al., 2011), and in-situ star formation in the ICM (Puchwein et al., 2010; Tonnesen and Bryan, 2012). A detailed discussion on the origin and growth of the ICL can be found in, e.g., Mihos et al. 2017 and Contini 2021. Moreover, the mass distribution of ICL has been observed to follow the global DM distribution, both in observations (e.g. Montes and Trujillo, 2019) and simulations (e.g. Alonso Asensio et al., 2020), making ICL a potential luminous tracer of the host DM halo mass distribution. To improve our understanding of the

[3]For ease of referring, I will use ICL to generally refer to this component in both groups and clusters.

growth of ICL, group-mass haloes provide an excellent link between galaxy and cluster haloes. Another interesting question is the formation timescale of ICL. Some recent studies have found ICL at $z > 1$ clusters and protoclusters, providing new insights about structure formation at such early epochs (e.g. Joo and Jee, 2023; Werner et al., 2023). One common finding from these works is that preprocessed free-floating stars from accreted haloes contributed more to the ICL than gradually stripped stars from orbiting satellite galaxies at $z > 1$, supporting the scenario that the dominant ICL production occurs concurrently with the growth of the central galaxies in high-redshift clusters. Despite the recent advancements in the study of ICL, there is much to be discovered about what we can learn from ICL about galaxy assembly and hierarchical structure formation, including the contribution of the stars in IGL/ICL to the total baryonic mass of the host systems, whether they can actually be used as a luminous tracer of the cluster halo, which processes are the dominant contributor to the ICL at different redshifts, and what can these processes imply about the formation history of galaxy clusters and their central galaxies.

State-of-the-art telescopes (e.g., JWST) and future surveys (e.g., *Euclid*, LSST of the Rubin Observatory) are going to provide deeper photometric and spectroscopic data from large areas in the sky, which will enable us to push boundaries in high-redshift and low-surface-brightness observations of galaxy groups and clusters. One major contribution from these next-generation wide surveys will be increasing the sample size of available galaxy groups and clusters by many times compared to currently available data. A larger sample size will improve the precision of our measurements and, therefore, enable more confident conclusions from the studies. Wide surveys in the infrared bands will help us study the high-redshift Universe in greater detail, enabling the development of a more informed timeline of cosmic events. Deeper photometric data will improve the LSB measurements, including IGL/ICL, and a large sample with deep data will enable us to perform statistical analysis of these components. All of these will provide better empirical constraints on galaxy and large-scale structure formation. However, to maximise the utility of these improved observations, it is crucial to develop improved tools to test galaxy formation theories against the observations, one of which is cosmological hydrodynamic simulations.

## 1.5 Cosmological Hydrodynamic simulations

Explaining the rich diversity of the galaxy population and characteristics from modern astronomical surveys across different environments over cosmic time with a compre-

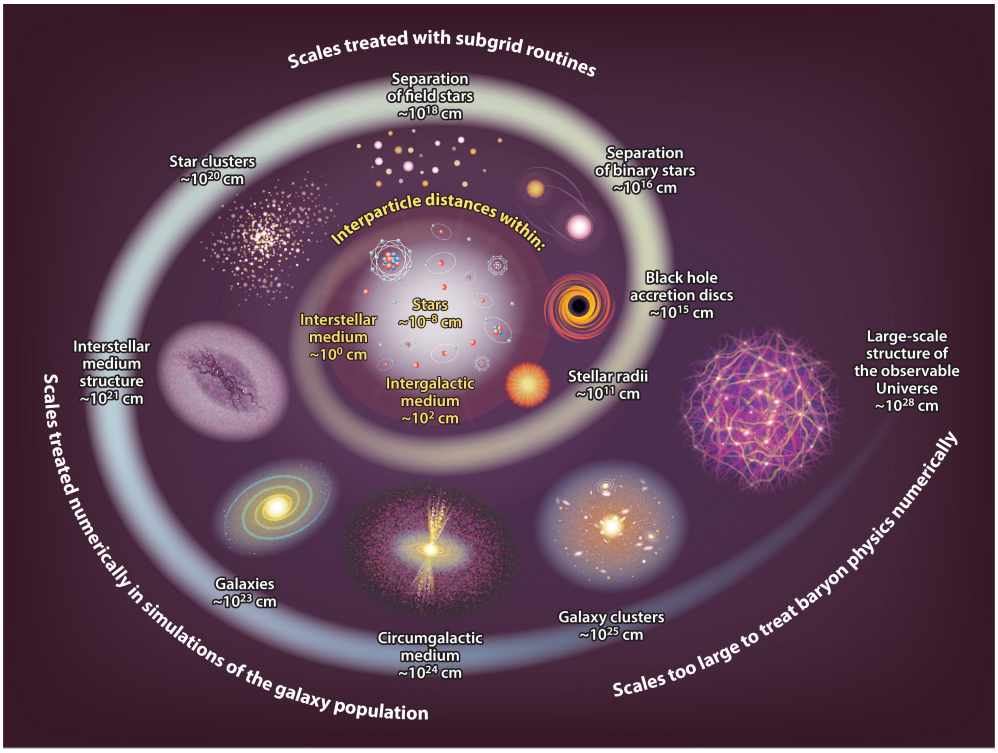


**Figure 1.2:** An illustration of the large dynamic range of length scales of processes that are relevant to galaxy formation and how they are modelled in hydrodynamic simulations. Figure from Crain and van de Voort (2023).

hensive theory of galaxy formation is a complex challenge due to its intrinsic multi-scale and multi-physics nature. However, the growth of DM haloes from cosmological initial conditions and the formation of galaxies within them is possible to model using numerical simulations. In particular, hydrodynamic simulations of representative cosmological volumes have been the most successful tool so far to involve DM and ordinary (or baryonic) matter that comprises gas, dust, and stars in the context of galaxy formation. For recent reviews on cosmological simulations and galaxy formation models, see e.g., Vogelsberger et al. (2020) and Crain and van de Voort (2023). Here, I am providing a short introduction on what are the building blocks of such simulations, what kinds of data products we obtain from these, and the performance of such simulations in explaining observed galaxy properties.

The framework of galaxy formation models is based on the cosmological model of the Universe (an overview of the building blocks of cosmological simulation is provided in Fig 1.3). In the ΛCDM cosmology, the DM distribution provides the skeleton of the large-scale structure formation. To capture structure formation in a cosmological volume—at least of the order of $(100\ \mathrm{Mpc})^3$—to star formation within galaxies from cold molecular gas, such simulations need to cover a very wide range of dynamic scales. However, it is computationally impossible to build these models entirely from first principles for the extremely large range of scale that needs to be covered. The only solution for this problem is to use subgrid physics models for processes that originate on smaller scales, including gas cooling, star formation, and the energy and momentum injection caused by supermassive black holes and massive stars. Figure 1.2 (Crain and van de Voort, 2023) illustrates the scale ranges of different physical processes and how they are tackled in such simulations.

Stars form due to the radiative cooling and gravity-induced condensation of gas. therefore, hydrodynamic simulation codes must allow for such a transformation from gas into stars. The cooling of gas particles is usually modelled by utilising pre-calculated and tabulated heating and cooling rates as a function of the redshift, temperature, density, and metallicity of the gas distribution (e.g. Wiersma et al., 2009; Ploeckinger and Schaye, 2020). The conversion of cold and dense gas into stars is applied as a stochastic process when the gas density exceeds a critical value (e.g. Schaye, 2004; Schaye and Dalla Vecchia, 2008). As the stellar population evolves, the associated stellar feedback to the galaxies and their CGM is modelled to replicate stellar winds and supernovae (e.g. Wiersma et al., 2009). In general, galaxy-scale stellar feedback is modelled by heating up the stellar surrounding either thermally or kinetically, therefore dispersing and ionizing the star-forming gas around stars. Additionally, stellar feedback enriches the chemical composition of the interstellar medium (ISM) by mixing-in metals that were synthesized in the stars. In the low-mass ($\leq 10^{10}\mathrm{M}_\odot$) galaxy population, stellar feedback is observed to regulate the star formation (by preventing extreme starburst at high redshift), and therefore, getting the stellar feedback right is necessary to reproduce the low-mass end of the observed galaxy stellar mass function (e.g. Puchwein and Springel, 2013).

Almost all galaxies with stellar mass $\geq 10^{10}\mathrm{M}_\odot$ are observed to have a central supermassive black hole (SMBH). In hydrodynamic simulations, the seeds of such black

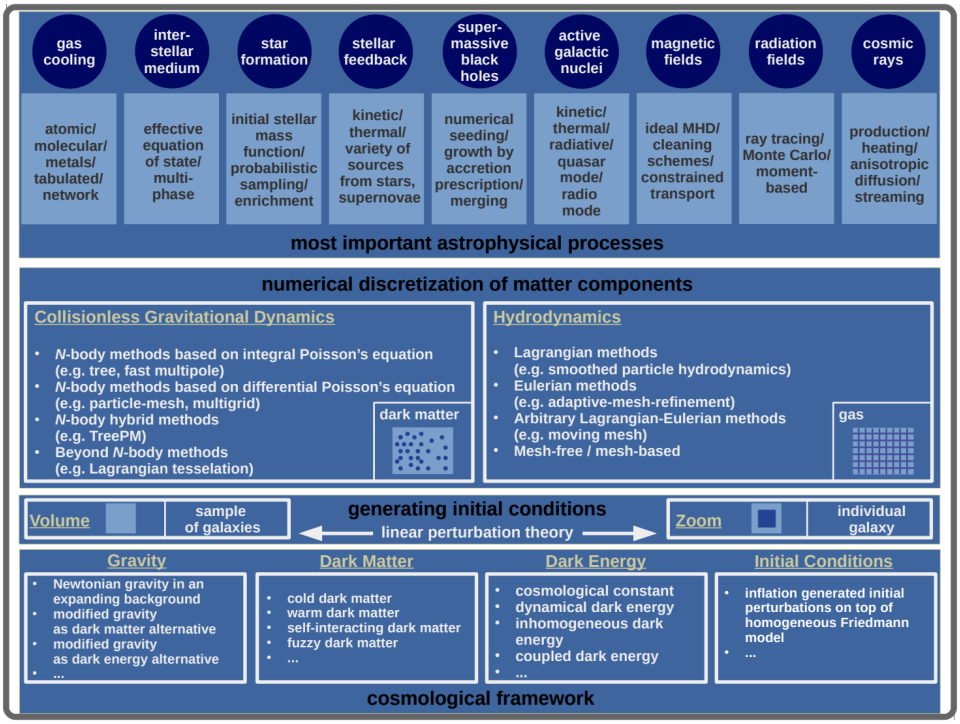


**Figure 1.3:** An overview of the primary ingredients of cosmological simulations. The ingredients are shown in a logical order from the bottom to the top of the figure, such that, the process starts from a given cosmological framework and follows from generating initial conditions to including the subgrid physics models. This is figure 2 from Vogelsberger et al. (2020).

holes are added following some empirical prescription because the formation mechanism of these SMBHs is still poorly understood. These black holes then grow via gas accretion and merging with other black holes (e.g. Bahé et al., 2022). During this accretion, the active galactic nucleus generates electromagnetic radiation, relativistic jets, and non-relativistic outflows, which are collectively referred to as the AGN feedback. Although only a fraction (likely small and unconstrained) of the AGN feedback couples with the surrounding gas, it regulates the black hole growth and star formation in massive haloes ($M_h \geq 10^{12}\mathrm{M}_\odot$, e.g., Booth and Schaye 2009). The AGN feedback plays an important role in reproducing the high-mass end of the observed galaxy stellar mass function (e.g. Puchwein and Springel, 2013). However, all the existing AGN feedback models are still quite over-simplified and have different issues in the entropy profiles of the ICM gas (see e.g. Oppenheimer et al., 2021; Altamura et al., 2023).

Along with these fundamental processes for galaxy formation, the physics of interstellar medium and dust, cosmic rays, magnetic field, and radiative transfer are also implemented in some recent simulations or are in the process of being implemented to achieve a more detailed evolution of galaxies in the cosmological context. The subgrid parameters whose values are unknown are now usually calibrated to match some reference observed quantity in the local Universe, such as the stellar mass function or the stellar-to-halo-mass. However, the highly non-linear relations between the subgrid model parameters and the simulated galaxy characteristics imply that calibration on one matched observable does not necessarily translate to reproducing any non-calibrated observable. Therefore, the validity of simulations to predict realistic observables should be subjected to multi-level and carefully designed checks.

Due to the required compromise between the spatial resolution and size of the simulation region, standard high-resolution cosmological simulation box sizes are around $(100\ \mathrm{Mpc})^3$. This size is too small for a statistical sample of massive galaxy clusters, whereas large simulation boxes in the order of $\mathrm{Gpc}^3$ volumes have a poor spatial resolution compared to what is necessary to study galaxy evolution within group and cluster mass haloes. A solution to this problem is the use of 'zoom-in simulation', where targets of interest (galaxies or clusters) are selected from a large-volume low-resolution simulation box. Then these smaller volumes are re-run with much higher resolution while the boundary conditions are taken from the large low-resolution box.

After running such simulations, the primary outputs from the simulations are usually multi-level particle data at a set of redshift stamps or 'snapshots'. Then the particle data goes through different post-processing to be ready to use for validity checks and comparison with observation. One fundamental step of such post-processing is

using a halo-finder code, e.g. SUBFIND (Springel et al., 2001; Dolag et al., 2009) or VELOCIraptor (Elahi, 2013; Elahi et al., 2019) to identify gravitationally bound haloes and self-bound subhaloes within them. Usually, some information is directly recoverable from simulation output, including particle ID, mass, and instantaneous velocities of the star, gas, DM, and black hole particles at each redshift stamp. Using this information and outputs from the halo-finder, high-level catalogues of galaxies and systems of galaxies (groups and clusters) can be produced, which include different properties such as their stellar and halo mass at different apertures, stellar age, star-formation rate, half mass radius, metallicity. Producing even higher-level data, such as multi-band photometry and spectra, requires forward modelling and is not always a part of a standard simulation data release. The key takeaway from understanding the data produced from simulations is that any property of an object in a simulation output catalogue can have many definitions, e.g., the stellar mass of a galaxy can be measured in different apertures. Also, as the SNR in simulation output is practically infinite, this is not directly comparable to any observational data without testing the effect of different types of noises and uncertainties that affect both simulated and observational data.



### 1.5.1 Current state of the field

Over the last decade, the capacity of hydrodynamic simulations to reproduce different properties of observed galaxy populations has significantly improved. A successful galaxy formation model should be ideally able to reproduce the fundamental properties of galaxies, such as their intrinsic luminosities, stellar and halo masses, sizes (half-mass or half-light radii), morphologies, metal abundances, stellar age, star formation rate, and gas content. While there is still scope for improvement, multiple flagship-scale simulations have been studied in detail and have been successful to various degrees in reproducing several observables of the galaxy population. These simulations include Illustris (Genel et al., 2014; Vogelsberger et al., 2014), Magneticum (Hirschmann et al., 2014), EAGLE (Schaye et al., 2015; McAlpine et al., 2016), Romulus (Tremmel et al., 2017), Horizon-AGN (Dubois et al., 2014; Kaviraj et al., 2017), IllustrisTNG (Nelson et al., 2018; Pillepich et al., 2018), and SIMBA (Davé et al., 2019). Figure 1.4 provides a visual representation of some of these recent simulations. The properties of the observed galaxy population that these simulations have been broadly successful in reproducing include the global stellar mass functions at $0 < z < 7$ (Furlong et al.,

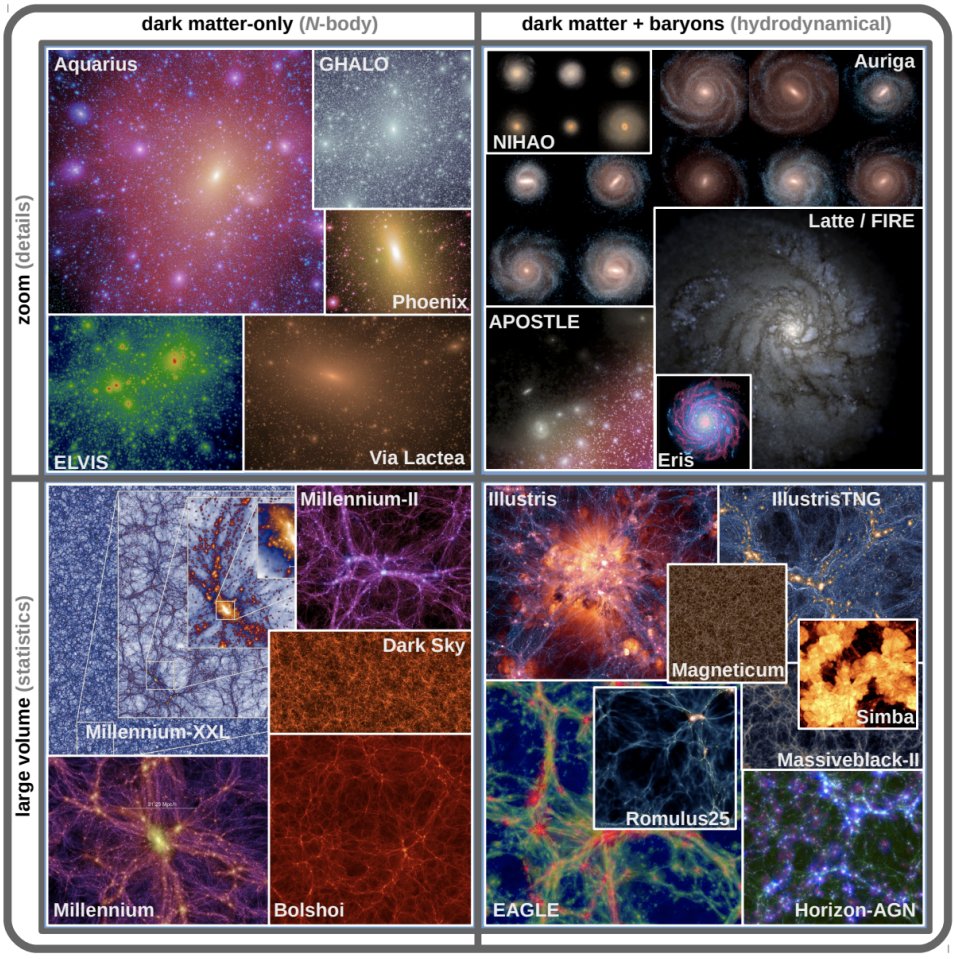


**Figure 1.4:** Visual representations from some recent simulations to illustrate their performance. The figure is divided in terms of their inclusion of dark matter only (N-body) and dark + baryonic matter from left to right; and between large volume and zoom simulations from bottom to top. Figure 1 from Vogelsberger et al. (2020).

2015; Pillepich et al., 2018; Davé et al., 2019), galaxy clustering (Artale et al., 2017; Crain et al., 2017; Springel et al., 2018), galaxy colours (Trayford et al., 2015, 2017; Nelson et al., 2018), and different scaling relations including the mass-metallicity relation (e.g., Lagos et al. 2016; Davé et al. 2019; Torrey et al. 2019, the Tully-Fisher relation (e.g., Vogelsberger et al. 2014; Ferrero et al. 2017; Sales et al. 2017, and the star-forming main sequence. For a detailed comparison of these simulations in reproducing different observables, see recent reviews by Vogelsberger et al. (2020) and Crain and van de Voort (2023).



While a lot of these aforementioned properties are broadly reproduced in the simulations, on a quantitative level, there is ample room for improvement. One general limitation in all the current simulations is that the subgrid models for supernovae and AGN feedback strongly affect their prediction of different galaxy properties. Given the complexity and our incomplete understanding of these feedback processes, these are usually modelled with simplified subgrid prescriptions, and their performance in different state-of-the-art simulations has degeneracy. These simulations also have a limited capacity to reproduce the internal and vertical structures of galaxies. Moreover, certain physical processes that can affect galaxy evolution significantly in different regimes are yet to be implemented, including the effects of magnetic fields (only implemented in IllustrisTNG so far), cosmic rays, thermal conduction, UVB radiation field (especially affecting galaxy evolution at the epoch of re-ionization), multi-phase CGM (cool gas and interface between cool and hot CGM), and local variation of radiation fields. For the next-generation simulations, a lot of effort is focused on incorporating these missing physics models with finer details, pushing the resolution limits, employing machine learning and AI to calibrate the subgrid models more efficiently, and probing larger volumes to be applicable to compare with high-redshift data from JWST and large-volume galaxy surveys like Euclid and LSST.

In this thesis, I have used the $(50\ \mathrm{Mpc})^3$ volume run of the EAGLE simulation and the Hydrangea simulations (Bahé et al., 2017), a suite of 24 high-resolution zoom-in simulations of massive (up to $> 10^{15}\mathrm{M}_\odot$ at $z = 0$) galaxy clusters and their large-scale surroundings. The Hydrangea simulations were run using the same variation of the EAGLE code that was used for the EAGLE volume used here. So far, the Hydrangea simulations, which are also part of the 30 cluster-EAGLE simulations, are the largest sample of massive galaxy clusters with comparable high resolution, and they have been broadly successful in reproducing observed properties of galaxies in dense environments (Bahé et al., 2017; Barnes et al., 2017). Although the above-mentioned limitations of current simulations are present in both EAGLE and Hydrangea, these

are the best simulation pairs to study the impact of different environments on galaxy evolution. However, one point of concern is that the availability of simulation data does not necessarily imply their utility or validity to compare to observations and draw useful insights from this. Especially because these simulations, like all state-of-the-art simulations, were calibrated with certain observables at $z = 0$, their performance in reproducing higher-redshift observations must be tested carefully before drawing any conclusions. Also, due to the coarse treatment of the subgrid physics models, just because the simulations reproduce an observable, it does not imply that it could replicate the physical processes leading to the observable as it occurs in the real Universe. That is why careful comparison of the simulated data to observational data is crucial along with the development of such sophisticated simulations.

## 1.6 Detailed comparison between simulations and observations

In recent years, multiple works (e.g. Bahé et al., 2021; Font et al., 2022) have shown that while comparing simulations to observations, subtle details in the analysis methods can strongly influence the conclusion of the analysis. A more reliable methodology requires an understanding of the nature of the data from both simulations and observations, and of the biases that may be included from either side of the data processing pipeline. A carefully designed comparison serves two major purposes: firstly, it enables us to test and improve the credibility of the simulations and their physics models. Secondly, it enables us to explain the physical processes that result in the observed properties of galaxies.

To illustrate the need for detail-oriented comparison, an example could be the comparison of mass and light between simulations and observations. In observations of galaxies, our primary data is the photons we get from these systems. To estimate the mass of a galaxy from the light, we need to make many assumptions about which environments those photons passed through, how much of that light was absorbed in cold gas clouds inside and outside of the Milky Way galaxy, what is the typical luminosity of different types of stars, what are the initial mass function and star-formation rate in the galaxy, and which distribution of age, metallicity, and type of stars can contribute to the combined spectral energy distribution and multi-band luminosity of the observed galaxy. All of these assumptions are physically motivated from detailed studies of each of these phenomena. However, even physically motivated

assumptions are subjected to the limitation of available information from the data and limitations in our understanding of these processes. On the other hand, in simulations, getting the mass is fairly straightforward because we have information about the mass of each type of particle that are gravitationally bound in a system. However, whether the mass inferred from observations is the same definition of mass we calculate by adding the particle masses does not have a simple answer due to the difference in the processes they are measured from and the potential biases and uncertainties they have. One may wonder, then, why we do not convert the mass from simulations to the light we may obtain from them at a comparable distance and environment to the observations. It is possible and is being done in multiple recent works. However, this process is again subject to all the above-mentioned assumptions in the physical processes that we have in converting light to mass. Explaining this complex process is not to discourage such attempts but, on the contrary, to demonstrate that we must take as detailed steps as possible to make sure that the data from simulations and observations are as similar as possible to make any conclusion and insight derived from such comparisons useful.

Another important point of concern is that the simulations are calibrated to match properties in the local Universe. It is quite possible that the good performance of all of the current state-of-the-art simulations in reproducing different properties at $z = 0$ is somewhat influenced by the calibration, and their data at higher redshifts are only numerical relics and unsuitable to be used to test galaxy formation theories at relevant epochs. Already existing tests of some properties at higher redshifts from some simulations show promising performance. However, we need to test their validity in much more detail at higher redshifts to confirm their credibility or lack thereof at such redshifts.

To summarise, state-of-the-art cosmological simulations can now reproduce fundamental properties of observed galaxies (e.g., the total stellar mass, stellar mass function) with unprecedented accuracy both in the local Universe and over more than half of the age of the Universe. Moreover, the next generation of simulations with improved physics models, better resolution, and larger cosmological volumes are underway. At the same time, state-of-the-art observational facilities (and next-generation survey instruments) are now (and getting ready for) producing deeper and higher-resolution data. This tremendous progress in both theory and observational sides implies that the measurement error will be low enough that systematics in the methodology will be the limiting factor in the conclusions we draw from comparing them. Therefore, now is the perfect time to build systems that improve the quality of insights we can

obtain from such comparisons.

## 1.7 Thesis outline



In this thesis, we compare different properties of galaxies in groups and clusters from the Hydrangea and EAGLE simulations to recent observations across $0 < z < 3.5$. We design these comparisons such that we start with broad properties, like the total stellar mass in groups and clusters, before we move on to more detailed properties, such as the spatial distribution of mass in galaxies within the clusters, the intragroup and intracluster light, and processes that quench massive galaxies at high redshifts ($z > 1$). We also prepare mock observations from simulations that are matched with deep imaging surveys such as the Kilo-Degree Survey (KiDS, De Jong et al., 2013; Kuijken et al., 2019) before we compare observables between them. By comparing a wide range of galaxy and host system properties from cosmological hydrodynamic simulations to recent high-quality observations of galaxy groups and clusters, we test the validity of the simulations at higher redshifts, and demonstrate how such comparisons can motivate new tests and provide novel insights about galaxy evolution in dense environments.

In **Chapter 2**, we compared different properties of massive galaxy clusters ($M \geq 10^{14}\mathrm{M}_{\odot}$ at $z$=0) from the Hydrangea simulation suite to recently observed data from different galaxy cluster studies out to $z$=2. We first confirmed that the total stellar mass in the Hydrangea clusters at a fixed halo mass and redshift is comparable to observed clusters in our tested redshift range. In a following test, we produced synthetic observations of galaxy clusters from Hydrangea and confirmed that the galaxy stellar mass from simulations within 30 kiloparsecs is a reasonable estimate of their observable stellar mass. Checking the dependency of the galaxy stellar mass function (SMF) on cluster halo mass showed that, at a fixed redshift, the normalization of cluster SMF strongly correlates with the cluster halo mass. Consequently, with a matched halo mass distribution to an observed cluster sample, the simulations predicted the observed SMF well out to $z$=1.5, which was not evident before matching the halo masses. We then studied the density profiles of clusters at $0 < z < 2$, for both the DM and stellar masses. By comparing the concentration parameters from the fitted Navarro-Frenk-White (NFW) profiles to previous observation-based works, this work verified that the opposite evolution of the DM and stellar concentration in clusters over cosmic time is not in tension with the ΛCDM cosmology. These findings illustrate how paying attention to detail changes our conclusions in such comparisons.

In **Chapter 3**, we studied a subtle but significant observable property of clusters, the intragroup or intracluster light (IGL or ICL). There has been an increasing effort in recent years to understand the origin and distribution of this diffuse light in systems of different halo masses. However, there was a gap between the simulation-based works (tracing mass distribution), and observation-based works (tracing light distribution). To bridge this gap, we created multi-band synthetic observations of ∼500 galaxy groups and clusters from the Hydrangea simulations, and matched the systematics to the Kilo Degree Survey (KiDS) and Galaxy and Mass Assembly (GAMA) survey data to which we compared the analysis from the work in the following chapter. This work resolved one crucial problem in the stacking analysis of IGL - selecting the best centre of the group on which that stacking will be performed. We found that selecting the galaxy with the highest associated halo mass as the central group galaxy, instead of the brightest galaxy, gives the best estimation. Also, instead of stacking groups from a large halo mass range, binning them by central galaxy luminosity provided a better understanding of the IGL growth. Finally, studying the colour, mass, and metallicity profiles of the diffuse light in groups and clusters from Hydrangea indicated that in low-mass groups, the IGL is predominantly accumulated by major mergers, whereas in more massive clusters, the main channel of ICL growth is via accretion of stripped stars from satellites.

The foundations of **Chapter 4** were based on the insights from **Chapter 3**, where we measured the IGL fraction in galaxy groups from KiDS+GAMA survey data and compared these results to the findings from **Chapter 3**. The standard data-processing pipeline for large cosmological imaging surveys, such as KiDS, is optimised to detect small, faint galaxies and measure their positions, fluxes, and shapes but not to retain the diffuse light in IGL/ICL at extended radii. We developed a special pipeline to re-process the KiDS survey images to optimise their use for diffuse light analysis and obtained the first robust measurement of IGL from a large group sample (850×5 exposures) down to 31-32 mag/arcsec$^2$. We found that systematics in the imaging data can affect IGL measurements even with our special-purpose pipeline. However, with a large sample and carefully optimised analysis, we can place well-constrained upper and lower limits on the IGL fraction for our group ensemble across redshifts $0.09 \leq z \leq 0.27$ and halo-masses $12.5 \leq \log_{10}[M_{200}/\mathrm{M}_\odot] \leq 14.0$. Our measurements are compatible with existing measurements of IGL in individual systems at similar redshift and halo mass ranges, however, with better constraints in the range of IGL fraction for the advantage of stacking. This work shed light on the potential performance of statistical analysis of diffuse light in large samples of groups and clusters from next-generation

observational programs like *Euclid* (Troja et al., 2023) and LSST (Ivezić et al., 2019). Moreover, the developed pipeline can be applied to the data from these surveys with minimum modification when that data is available.



In **Chapter 5**, we explored the potential of an environment-dependent halo mass function as a driver for the early quenching of $z \geq 1.5$ cluster galaxies. Recent works have found that a fraction of the intermediate-mass galaxies ($10^{10}\mathrm{M}_{\odot} \leq M_{*} \leq 10^{11}\mathrm{M}_{\odot}$) in galaxy clusters are already quenched by $z \sim 1.5$. This is very puzzling as the clusters were not yet completely formed by that time and therefore, the known quenching mechanisms that work in clusters could not be strong enough. Moreover, these massive quenched galaxies have stellar populations of similar age in both clusters and the field. This suggests that the dominant quenching mechanism for massive galaxies is similar in both environments. In this work, we used data from the Hydrangea and EAGLE simulations to test whether this early quenching of massive galaxies in $z \geq 1.5$ clusters results from fundamental differences in their halo properties compared to the field. We found that at $10^{10} \leq M_{\star}/\,\mathrm{M}_{\odot} \leq 10^{11}$, quenched fractions in the redshift range $1.5 < z < 3.5$ are consistently higher for galaxies with higher peak maximum circular velocity of the dark matter halo ($v_{\mathrm{max,peak}}$). We also found that the distribution of $v_{\mathrm{max,peak}}$ is strongly biased towards higher values for cluster satellites than the field centrals. Due to this difference in the halo properties of cluster and field galaxies, secular processes alone may account for (most of) the environmental excess of massive quenched galaxies in high-redshift (proto) clusters. Taken at face value, our results challenge a fundamental assumption of popular quenching models, namely that clusters are assembled from an unbiased subset of infalling field galaxies. If confirmed, this would imply that such models must necessarily fail at high redshift, as indicated by recent observations. This work identifies a new way to examine the effects of environment and internal processes in quenching massive galaxies at high redshift.

Along with the above chapters, I have worked as a part of the low-surface-brightness working group of the Legacy Survey of Space and Time (LSST) collaboration of the Vera Rubin Telescope, where we predicted the fraction and other measurements of the ICL in galaxy clusters (halo mass$\sim 10^{14}\mathrm{M}_{\odot}$) by applying different observational methods in LSST-like mock observations. These mock observations were created from multiple cosmological hydrodynamic simulations - Hydrangea, IllustrisTNG, Horizon-AGN, and Magneticum. These predictions from matched synthetic observations will be crucial to optimize the utility of the large volume of exceptional data from the upcoming LSST survey. This collective effort also shed light on whether simulators

and observers measure the same component while studying ICL and possible reasons behind any match or lack thereof in these approaches. The manuscript from this work is currently under review in the journal 'Monthly Notices of the Royal Astronomical Society'.



# References


Allen, S. W., Evrard, A. E., and Mantz, A. B., 2011, ARA&A, 49, 409
Alonso Asensio, I., Dalla Vecchia, C., Bahé, Y. M., et al., 2020, MNRAS, 494, 1859
Alpher, R. A., Bethe, H., and Gamow, G., 1948, Physical Review, 73, 803
Altamura, E., Kay, S. T., Bower, R. G., et al., 2023, MNRAS, 520, 3164
Artale, M. C., Pedrosa, S. E., Trayford, J. W., et al., 2017, MNRAS, 470, 1771
Bahé, Y. M., Schaye, J., Schaller, M., et al., 2021, arXiv e-prints, arXiv:2109.01489
Bahé, Y. M., Schaye, J., Schaller, M., et al., 2022, MNRAS, 516, 167
Bahé, Y. M. et al., 2017, MNRAS, 470, 4186
Balogh, M. L., Gilbank, D. G., Muzzin, A., et al., 2017, MNRAS, 470, 4168
Balogh, M. L., Navarro, J. F., and Morris, S. L., 2000, ApJ, 540, 113
Balogh, M. L., van der Burg, R. F. J., Muzzin, A., et al., 2021, MNRAS, 500, 358
Balogh, M., Morris, S., and Yee, H., 1999, ApJ, 527, 54,
Barnes, D. J., Kay, S. T., Bahé, Y. M., et al., 2017, MNRAS, 471, 1088
Bekki, K. and Couch, W. J., 2011, MNRAS, 415, 1783
Bennett, C. L., Banday, A. J., Gorski, K. M., et al., 1996, ApJL, 464, L1
Bennett, C. L., Halpern, M., Hinshaw, G., et al., 2003, ApJS, 148, 1
Blanton, M. R., Eisenstein, D., Hogg, D. W., et al., 2005, ApJ, 629, 143
Boselli, A., Fossati, M., and Sun, M., 2022, A&AR, 30, 3
Boselli, A. and Gavazzi, G., 2006, Publications of the Astronomical Society of the Pacific, 118, 517
Brown, T., Catinella, B., Cortese, L., et al., 2017, MNRAS, 466, 1275
Byrd, G. and Valtonen, M., 1990, ApJ, 350, 89
Colless, M., Dalton, G., Maddox, S., et al., 2001, MNRAS, 328, 1039
Contini, E., 2021, Galaxies, 9, 60
Crain, R. A., Bahé, Y. M., Lagos, C. d. P., et al., 2017, MNRAS, 464, 4204
Crain, R. A. and van de Voort, F., 2023, Annual Review of Astronomy and Astrophysics, 61, 473
Davé, R., Anglés-Alcázar, D., Narayanan, D., et al., 2019, MNRAS, 486, 2827
Delos, M. S. and White, S. D. M., 2023, MNRAS, 518, 3509
DeMaio, T., Gonzalez, A. H., Zabludoff, A., et al., 2018, MNRAS, 474, 3009
DeMaio, T., Gonzalez, A. H., Zabludoff, A., et al., 2020, MNRAS, 491, 3751
Dicke, R. H., Peebles, P. J. E., Roll, P. G., et al., 1965, ApJ, 142, 414
Dolag, K., Borgani, S., Murante, G., et al., 2009, MNRAS, 399, 497
Dressler, A., 1980, ApJ, 236, 351
Dubois, Y., Pichon, C., Welker, C., et al., 2014, MNRAS, 444, 1453
Einasto, J., 2013, Brazilian Journal of Physics, 43, 369
Elahi, P. J. (June 2013). *STF: Structure Finder*. Astrophysics Source Code Library, record ascl:1306.009. ascl: 1306.009.
Elahi, P. J., Poulton, R., and Canas, R. (Nov. 2019). *VELOCIraptor-STF: Six-dimensional Friends-of-Friends phase space halo finder*. Astrophysics Source Code Library, record ascl:1911.020. ascl: 1911.020.
Fabello, S., Kauffmann, G., Catinella, B., et al., 2012, MNRAS, 427, 2841
Ferrero, I., Navarro, J. F., Abadi, M. G., et al., 2017, MNRAS, 464, 4736
Font, A. S., McCarthy, I. G., Belokurov, V., et al., 2022, MNRAS, 511, 1544
Friedman, A., 1922, Zeitschrift für Physik, 10, 377
Furlong, M., Bower, R. G., Theuns, T., et al., 2015, MNRAS, 450, 4486

## 1.7. REFERENCES


Gallagher John S., I. and Ostriker, J. P., 1972, Astronomical Journal, 77, 288
Genel, S., Vogelsberger, M., Springel, V., et al., 2014, MNRAS, 445, 175
Giovanelli, R and Haynes, M., 1985, ApJ, 292, 404
Gunn, J. E. and Gott J. Richard, I., 1972, ApJ, 176, 1
Guo, Q., White, S., Boylan-Kolchin, M., et al., 2011, MNRAS, 413, 101
Guth, A. H., 1981, Physical Review D, 23, 347
Hess, K. M. and Wilcots, E. M., 2013, Astronomical Journal, 146, 124
Hirschmann, M., Dolag, K., Saro, A., et al., 2014, MNRAS, 442, 2304
Hubble, E., 1929, Proceedings of the National Academy of Science, 15, 168
Ivezić, Ž., Kahn, S. M., Tyson, J. A., et al., 2019, ApJ, 873, 111
Jiménez-Teja, Y., Dupke, R., Benítez, N., et al., 2018, ApJ, 857, 79
De Jong, J. T. A., Kuijken, K., Applegate, D., et al., 2013, The Messenger, 154, 44
Joo, H. and Jee, M. J., 2023, Nat., 613, 37
Kauffmann, G., White, S. D. M., Heckman, T. M., et al., 2004, MNRAS, 353, 713
Kaviraj, S., Laigle, C., Kimm, T., et al., 2017, MNRAS, 467, 4739
Kravtsov, A. V. and Borgani, S., 2012, ARA&A, 50, 353
Kuijken, K., Heymans, C., Dvornik, A., et al., 2019, A&A, 625, A2
Lagos, C. d. P., Theuns, T., Schaye, J., et al., 2016, MNRAS, 459, 2632
Larson, R. B., Tinsley, B. M., and Caldwell, C. N., 1980, ApJ, 237, 692
Lemaître, G. H. (Jan. 1927). "The Gravitational Field in a Fluid Sphere of Uniform Invariant Density, According to the Theory of Relativity." PhD thesis. Massachusetts Institute of Technology.
Martínez-Lombilla, C., Brough, S., Montes, M., et al., 2023, MNRAS, 518, 1195
McAlpine, S., Helly, J. C., Schaller, M., et al., 2016, Astronomy and Computing, 15, 72
McCarthy, I. G., Frenk, C. S., Font, A. S., et al., 2008, MNRAS, 383, 593
Merritt, D., 1983, ApJ, 264, 24
Mihos, C. (Aug. 2015). "Intragroup and Intracluster Light". *IAU General Assembly*. Vol. 29, 2247903, 2247903.
Mihos, J. C., Harding, P., Feldmeier, J., et al., 2005, ApJL, 631, L41
Mihos, J. C., Harding, P., Feldmeier, J. J., et al., 2017, ApJ, 834, 16
Mo, H., van den Bosch, F. C., and White, S. (2010). *Galaxy Formation and Evolution*.
Montes, M., 2022, Nature Astronomy, 6, 308
Montes, M., Brough, S., Owers, M. S., et al., 2021, ApJ, 910, 45
Montes, M. and Trujillo, I., 2014, ApJ, 794, 137
Montes, M. and Trujillo, I., 2018, MNRAS, 474, 917
Montes, M. and Trujillo, I., 2019, MNRAS, 482, 2838
Moore, B., Katz, N., Lake, G., et al., 1996, Nat., 379, 613
Moore, B., Lake, G., and Katz, N., 1998, ApJ, 495, 139
Murante, G., Giovalli, M., Gerhard, O., et al., 2007, MNRAS, 377, 2
Nelson, D., Pillepich, A., Springel, V., et al., 2018, MNRAS, 475, 624
Odekon, M. C., Koopmann, R. A., Haynes, M. P., et al., 2016, ApJ, 824, 110
Oort, J. H., 1932, Bulletin Astronomical Institute of the Netherlands, 6, 249
Oppenheimer, B. D., Babul, A., Bahé, Y., et al., 2021, Universe, 7, 209
Peacock, J. A. (1999). *Cosmological Physics*.
Peebles, P. J. E. and Yu, J. T., 1970, ApJ, 162, 815
Peng, Y.-j., Lilly, S. J., Kovač, K., et al., 2010, ApJ, 721, 193
Peng, Y.-j., Lilly, S. J., Renzini, A., et al., 2012, ApJ, 757, 4
Peng, Y., Lilly, S. J., Kovač, K., et al., 2010, ApJ, 721, 193
Penzias, A. A. and Wilson, R. W., 1965, ApJ, 142, 419
Perlmutter, S., Aldering, G., Goldhaber, G., et al., 1999, ApJ, 517, 565
Pillepich, A., Nelson, D., Hernquist, L., et al., 2018, MNRAS, 475, 648
Planck Collaboration, Aghanim, N., Akrami, Y., et al., 2020, A&A, 641, A6
Planck Collaboration XVI, 2014, A&A, 571, A16
Ploeckinger, S. and Schaye, J., 2020, MNRAS, 497, 4857
Press, W. H. and Schechter, P., 1974, ApJ, 187, 425

Puchwein, E. and Springel, V., 2013, MNRAS, 428, 2966
Puchwein, E., Springel, V., Sijacki, D., et al., 2010, MNRAS, 406, 936
Ragusa, R., Iodice, E., Spavone, M., et al., 2023, A&A, 670, L20
Riess, A. G., Filippenko, A. V., Challis, P., et al., 1998, Astronomical Journal, 116, 1009
Rubin, V. C., Ford W. K., J., and Thonnard, N., 1980, ApJ, 238, 471
Rubin, V. C. and Ford W. Kent, J., 1970, ApJ, 159, 379
Sales, L. V., Navarro, J. F., Oman, K., et al., 2017, MNRAS, 464, 2419
Schaye, J., 2004, ApJ, 609, 667
Schaye, J., Crain, R. A., Bower, R. G., et al., 2015, MNRAS, 446, 521
Schaye, J. and Dalla Vecchia, C., 2008, MNRAS, 383, 1210
Slipher, V. M., 1917, The Observatory, 40, 304
Springel, V., Pakmor, R., Pillepich, A., et al., 2018, MNRAS, 475, 676
Springel, V., White, S. D. M., Jenkins, A., et al., 2005, Nat., 435, 629
Springel, V., White, S. D. M., Tormen, G., et al., 2001, MNRAS, 328, 726
Tonnesen, S. and Bryan, G. L., 2012, MNRAS, 422, 1609
Torrey, P., Vogelsberger, M., Marinacci, F., et al., 2019, MNRAS, 484, 5587
Trayford, J. W., Camps, P., Theuns, T., et al., 2017, MNRAS, 470, 771
Trayford, J. W., Theuns, T., Bower, R. G., et al., 2015, MNRAS, 452, 2879
Tremmel, M., Karcher, M., Governato, F., et al., 2017, MNRAS, 470, 1121
Trimble, V., 2012, The Observatory, 132, 33
Trimble, V., 1987, ARA&A, 25, 425
Trimble, V., 2013, arXiv e-prints, arXiv:1307.2289
Troja, A., Tutusaus, I., Sorce, J., et al. (June 2023). "Euclid in a nutshell". *41st International Conference on High Energy physics*, 94, 94. DOI: 10.48550/arXiv.2211.09668. arXiv: 2211.09668 [astro-ph.IM].
van der Burg, R. F. J., Rudnick, G., Balogh, M. L., et al., 2020, A&A, 638, A112
Vogelsberger, M., Genel, S., Springel, V., et al., 2014, MNRAS, 444, 1518
Vogelsberger, M., Marinacci, F., Torrey, P., et al., 2020, Nature Reviews Physics, 2, 42
Webb, K., Balogh, M. L., Leja, J., et al., 2020, MNRAS, 498, 5317
Weinmann, S. M., Kauffmann, G., von der Linden, A., et al., 2010, MNRAS, 406, 2249
Weinmann, S. M., Van Den Bosch, F. C., Yang, X., et al., 2006, MNRAS, 372, 1161
Werner, S. V., Hatch, N. A., Matharu, J., et al., 2023, MNRAS, 523, 91
Wetzel, A. R., Tinker, J. L., and Conroy, C., 2012, MNRAS, 424, 232
White, S. D. M. and Rees, M. J., 1978, MNRAS, 183, 341
White, S. D. M. and Frenk, C. S., 1991, ApJ, 379, 52
Wiersma, R. P. C., Schaye, J., Theuns, T., et al., 2009, MNRAS, 399, 574
Wiersma, R. P., Schaye, J., and Smith, B. D., 2009, MNRAS, 393, 99
Willman, B., Governato, F., Wadsley, J., et al., 2004, MNRAS, 355, 159
Woo, J., Dekel, A., Faber, S. M., et al., 2012, MNRAS, 428, 3306
York, D. G., Adelman, J., Anderson John E., J., et al., 2000, Astronomical Journal, 120, 1579
Zhang, Y., Yanny, B., Palmese, A., et al., 2019, ApJ, 874, 165
Zibetti, S., White, S. D. M., Schneider, D. P., et al., 2005, MNRAS, 358, 949
Zwicky, F., 1933, Helvetica Physica Acta, 6, 110